# Spectroscopy of Mn-Doped Glasses of $CaO\text{-}Ga_2O_3\text{-}GeO_2$ System

[1,2]Padlyak B., [1]Vlokh O., [3]Kukliński B. and [4]SagooK.

[1]Institute of Physical Optics, 23 Dragomanov St., 79005 Lviv, Ukraine, e-mail:vlokh@ifo.lviv.ua
[2]Department of Physics, Kazimierz Wielki University of Bydgoszcz, 11 Weyssenhoff Sq., 85072 Bydgoszcz, Poland, e-mail: fizbp@ab.edu.pl
[3]Institute of Experimental Physics, University of Gdańsk, 57 Wita Stwosza St., 80952 Gdańsk, Poland
[4]Jobin Yvon IBH Ltd., 45 Finnieston St., G3 8JU Glasgow, UK

Received: 04.11.2005

## Abstract

The EPR, UV and visible optical spectra of absorption, luminescence excitation and emission, as well as the luminescence kinetics of impurity $Mn^{2+}$ centres in Mn-doped glasses of $CaO\text{-}Ga_2O_3\text{-}GeO_2$ system have been measured and analysed. The EPR spectra of as-synthesised Mn-doped glasses consist of three broad bands with the effective *g*-factors $g_{eff} \cong 4.3$, 3.0 and 2.0. The observed spectra have been attributed to both the isolated $Mn^{2+}$ ($3d^5$, $^6S_{5/2}$) ions occupying octahedral sites and revealing a broad distribution of crystal field parameters, as well as small clusters of $Mn^{2+}$ ions. The optical spectroscopy has shown that the manganese impurity is incorporated into octahedral sites of $CaO\text{-}Ga_2O_3\text{-}GeO_2$ glass network as both $Mn^{2+}$ and $Mn^{3+}$ ions. The intense broad absorption band with the maximum near 460 nm is related to the spin-allowed $^5E_g \rightarrow {}^5T_{2g}$ transition of $Mn^{3+}$ ions in trigonally distorted octahedral sites of $CaO\text{-}Ga_2O_3\text{-}GeO_2$ glass network. The weak spin-forbidden absorption lines of $Mn^{2+}$ ions have not been observed against the background of a strong absorption band of $Mn^{3+}$. The observed luminescence band with the maximum in the vicinity of 650 nm is explained by $T_{1g} \rightarrow {}^6A_{1g}$ transition of $Mn^{2+}$ ions occurring in trigonally distorted octahedral sites. The luminescence decay curve of $Mn^{2+}$ could be satisfactorily described within two-exponent approximation. The two different lifetimes ($\tau_1$ = 12.4 ms and $\tau_2$ = 3.98 ms at $\lambda_{exc}$ = 300 nm) correspond to the two types of $Mn^{2+}$ centres with different local environments. A possible local structure of different $Mn^{2+}$ centres in $CaO\text{-}Ga_2O_3\text{-}GeO_2$ glass network is discussed.

**Keywords:** germanate glasses; manganese ions; electron paramagnetic resonance; optical absorption; photoluminescence; luminescence decay

**PACS:** 42.70.Ce, 71.55.Jv, 76.30.Fc, 78.40.Pg, 78.55.Hx

## 1. Introduction

Disordered crystals and glass matrices doped with transition metal ions are still attractive as efficient phosphors and laser media, especially for tuneable solid state lasers. In particular, the crystals and glasses activated with $Mn^{2+}$ represent well-known materials for highly efficient (green or red) phosphors [1-3]. Contrary to crystals, spectroscopic properties and incorporation peculiarities of transition ions in a glass network are studied insufficiently. Therefore, experimental investigations and analysis of spectroscopic properties of the impurity transition ions in disordered compounds, particularly in compositionally (or

substitutionally) disordered oxide crystals and glasses, remain an urgent topic in the optical-material technology and solid state physics. This also concerns the manganese impurity, which could be introduced as $Mn^{2+}$, $Mn^{3+}$, $Mn^{4+}$ or $Mn^{5+}$ ions into different structural sites in oxide glasses and crystals and so could reveal various spectroscopic properties [4-6].

Modern optical and electron paramagnetic resonance (EPR) spectroscopic techniques provide powerful tools for studying the valence state, local environment symmetry and the crystal field parameters of the transition ions in compounds with both the ordered and disordered structures. The compounds that can be obtained in both the crystalline and vitreous (or glassy) phases are suitable objects for such the studies. We have selected for our measurements and analyses the compounds of ternary $CaO$-$Ga_2O_3$-$GeO_2$ system. Three stable crystalline forms exist in this system: $Ca_3Ga_2Ge_3O_{12}$ (the ordered garnet structure, space group *Ia3d*), $Ca_3Ga_2Ge_4O_{14}$ (substitutionally disordered Ca-gallogermanate structure, space group $P32_1$) and $Ca_2Ga_2GeO_7$ (gelenite structure, space group $P\bar{4}2_1m$) [7,8], together with the corresponding glassy (vitreous) forms possessing stoichiometric compositions similar to those of the above crystals [9]. The X-ray scattering and molecular dynamics simulation [10] have shown that the structure of undoped glasses with $Ca_3Ga_2Ge_3O_{12}$ and $Ca_3Ga_2Ge_4O_{14}$ compositions is characterised by a short-range chemical ordering, which is similar in the main to that happening in the corresponding crystalline compounds.

The results of the EPR and optical spectroscopies of manganese ions in the $Ca_3Ga_2Ge_3O_{12}$ and $Ca_3Ga_2Ge_4O_{14}$ single crystals have been earlier described in a number of works [11-15]. The EPR and optical spectroscopy data for the Mn-doped glasses of $CaO$-$Ga_2O_3$-$GeO_2$ system have been obtained for the first time in [16-18]. The EPR and optical spectra of the Mn-doped glasses with the $Ca_3Ga_2Ge_3O_{12}$ and $Ca_3Ga_2Ge_4O_{14}$ compositions have been measured and analysed there. In this work we discuss the mentioned spectra and the luminescence kinetics of $Mn^{2+}$ ions in the glasses of $CaO$-$Ga_2O_3$-$GeO_2$ system and compare them to the corresponding data obtained earlier for their crystalline analogues and the glasses of other systems. Basing on the analysis of those results, we examine a local structure of luminescence $Mn^{2+}$ centres in the $CaO$-$Ga_2O_3$-$GeO_2$ glass network.

## 2. Experimental details

### 2.1. Preparation and characteristics of the samples under study

Mn-doped glasses of $CaO$-$Ga_2O_3$-$GeO_2$ system of high chemical purity and optical quality characterised with different stoichiometric compositions were obtained in corundum crucibles, using the high-temperature synthesis technique [9]. Mn impurity was added into the glass composition as liquid $Mn(NO_3)_2$ and $Mn(CH_3COOH)_2$ solutions in the amounts of 0.001÷0.2 wt. %. Depending on the manganese content, the colour of the Mn-doped glasses obtained this way varied from pale to dark brown, respectively, for the Mn contents less and larger than 0.01 wt. %.

Chemical composition of the glasses was controlled with the X-ray microanalysis method, using "Camebax" apparatus. Structural investigations employing the X-ray scattering technique revealed that our Mn-doped glass samples with the $Ca_3Ga_2Ge_3O_{12}$ and $Ca_3Ga_2Ge_4O_{14}$ compositions manifested a typical glassy-like X-ray structure factor quite similar to that obtained for the undoped glass of the same composition [10]. Small traces of crystalline phases included into the basic glass material were observed in some investigated samples. We selected for further spectroscopic studies only Mn-doped glasses that included no crystalline precipitates and had the composition similar to that of calcium-gallium-germanium garnet ($Ca_3Ga_2Ge_3O_{12}$:Mn; the content of Mn

being 0.005, 0.01 and 0.2 wt. %) and Ca-gallogermanate ($Ca_3Ga_2Ge_4O_{14}$:Mn; 0.15 wt. % of Mn). We prepared the glass samples with the dimensions $5\times2\times1$ mm$^3$ for the EPR investigations. The samples for the optical measurements were cut to approximate size $8\times4\times2$ mm$^3$ and then thoroughly polished.

## 2.2. Experimental methods and equipment

The X-band EPR spectra were recorded with commercial computer-controlled RADIOPAN SE/X-2544 (Poznań, Poland) and AE-4700 (Lviv, Ukraine) radio-frequency spectrometers that employ 100 kHz magnetic field modulation at the temperatures 300 K and 77 K. The microwave frequency was controlled by means of diphenylpicrylhydrazyl (DPPH) *g*-marker ($g$=2.0036±0.0001).

Optical absorption spectra were measured at the room temperature with "Specord M-40" (Carl Zeiss Jena) spectrophotometer. Photoluminescence spectra were detected at 300 K and 85 K upon the frontal excitation and observation of the emission in sample, using the equipment built at the Condensed Matter Spectroscopy Division (Institute of Experimental Physics, University of Gdańsk). The emission spectra were corrected for spectral sensitivity of the equipment. Hanovia xenon lamp (P = 1000 W) was used as excitation source. The wavelengths required for the excitation and observation were selected with the aid of SPM-2 prism monochromator (Carl Zeiss Jena) that utilized stepping motors driven by computer. Photomultipliers used in the detection branch worked in the analogue or photon counter regime. In the latter case, they sent data to the computer *via* a digital boxcar system. Finally, Hamamatsu R928 photomultiplier was used as a detector.

The luminescence decays were studied at the room temperature and analysed using the IBH 5000U fluorescence lifetime system. We used the excitation source 5000XeF ($\lambda_{exc}$ = 275 and 300 nm) and the detector TBX-04A. Zero-order long band-pass filter at 590 nm was used for detecting the emission. The investigated sample was mounted on the front surface of sample holder.

## 3. Results and discussion

### 3.1. EPR spectroscopy of Mn-doped glasses of $CaO$-$Ga_2O_3$-$GeO_2$ system

The EPR spectra of as-synthesised Mn-doped $CaO$-$Ga_2O_3$-$GeO_2$ glasses consist of three broad bands with the effective *g*-factors equal to $g_{eff} \cong$ 4.3, 3.0 and 2.0 (see Fig. 1a). Six weakly resolved hyperfine-structure components due to $^{55}$Mn isotope (nuclear spin $I$ = 5/2, natural abundance 100%) are observed for the signal with $g_{eff} \cong 2.0$ (Fig. 1b). The intensity of all the EPR bands is approximately linearly related to the Mn content. The shapes and linewidths of the observed EPR bands are independent of temperature and basic glass composition. The bands are characterised with inhomogeneous broadening caused by structural disordering in glasses. The EPR spectra of Mn-doped glasses with the $Ca_3Ga_2Ge_3O_{12}$ and $Ca_3Ga_2Ge_4O_{14}$ compositions are virtually identical (see Fig. 1a and b).

The EPR spectra observed earlier in [15] have been attributed to both the isolated $Mn^{2+}$ ($3d^5$, $^6S_{5/2}$) ions and their small clusters that contain more than one $Mn^{2+}$ ion. Comparative analysis of the EPR spectra of $Mn^{2+}$ in the $CaO$-$Ga_2O_3$-$GeO_2$ glasses (see Fig. 1) and substitutionally disordered $Ca_3Ga_2Ge_4O_{14}$ crystals [14,15] shows that the isolated $Mn^{2+}$ ions occupy octahedral sites in the glass network and are characterised by a broad distribution of crystal field parameters. A comparison of the hyperfine-structure constants for $^{55}$Mn isotope in calcium-gallium-germanium garnet ($A_z$ = 82 G and $A_y$ = 85 G) [13], Ca-gallogermanate ($A_z$ = 91 G) [14,15] and the glasses of $CaO$-$Ga_2O_3$-$GeO_2$ system ($A$ = 75 ± 3 G) [16] evidences that the chemical bond of $Mn^{2+}$ ions with the ligands is ionic in crystals and partly covalent in their glassy analogues.

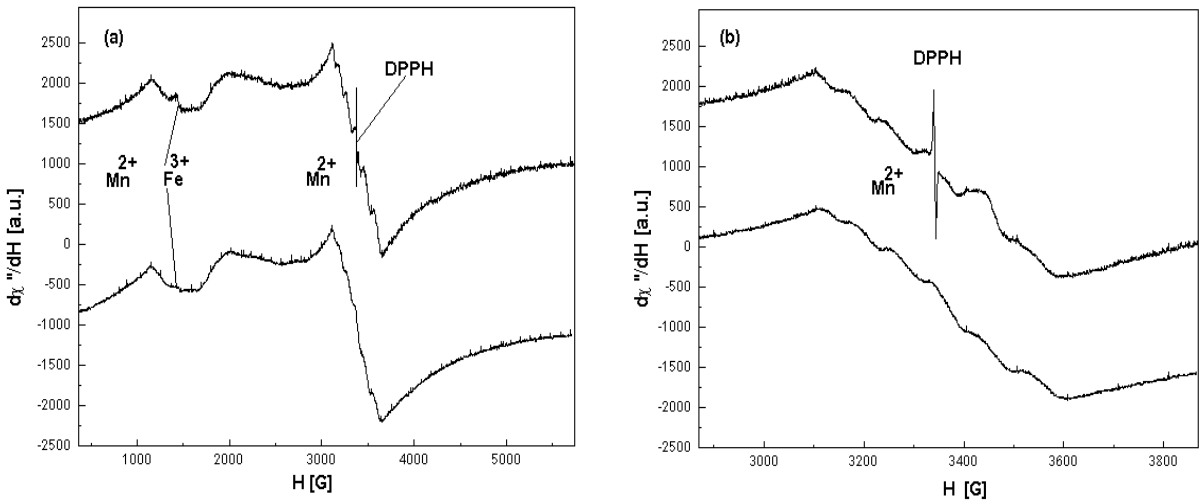


**Fig. 1.** X-band EPR spectra of the Mn-doped $CaO\text{-}Ga_2O_3\text{-}GeO_2$ glasses: the whole spectra (a) and their central regions (b). The upper spectra are recorded at 77 K for the glass with $Ca_3Ga_2Ge_3O_{12}$ composition containing 0.01 wt. % of Mn and the lower ones at 300 K for the glass with $Ca_3Ga_2Ge_4O_{14}$ composition containing 0.15 wt. % of Mn.

It should be emphasised that a weak EPR signal is observed at $g_{eff} \cong 4.29$ for the all Mn-doped $CaO\text{-}Ga_2O_3\text{-}GeO_2$ glasses (see Fig. 1a). This signal is typical for the glasses and the other disordered systems [19-20]. It may be assigned to the isolated $Fe^{3+}$ ($3d^5$, $^6S_{5/2}$) ions placed in the octahedrally and/or tetrahedrally coordinated sites with a strong rhombic distortion [21]. The amount of $Fe^{3+}$ ions in the investigated samples estimated by the EPR technique does not exceed $10^{-3}$ wt. %. This cannot change essentially the optical properties of Mn-doped glasses of $CaO\text{-}Ga_2O_3\text{-}GeO_2$ system.

### 3.2. Optical spectroscopy of Mn-doped glasses of $CaO\text{-}Ga_2O_3\text{-}GeO_2$ system

The undoped $CaO\text{-}Ga_2O_3\text{-}GeO_2$ glasses are transparent in the UV region down to 280÷300 nm (see Fig. 2a). The Mn-doped glasses with the $Ca_3Ga_2Ge_3O_{12}$ and $Ca_3Ga_2Ge_4O_{14}$ compositions are characterised by almost identical optical absorption spectra (Fig. 2b and c), which exhibit

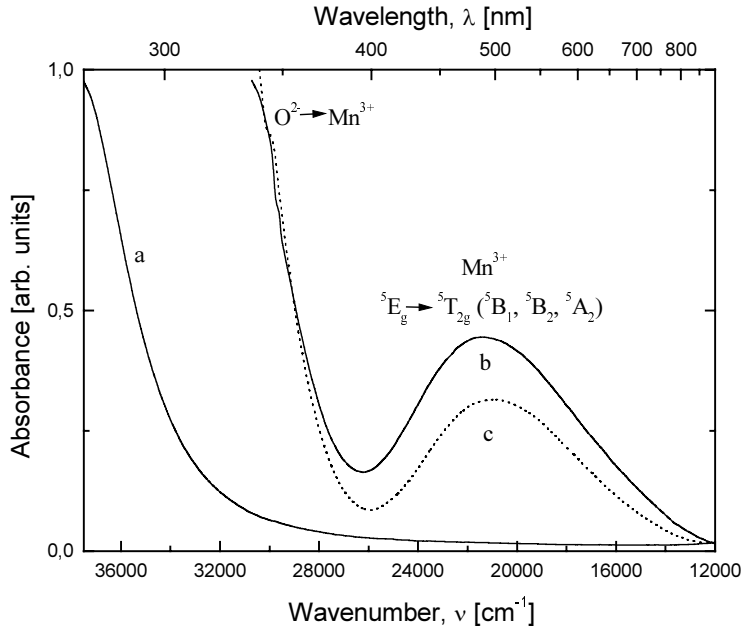


**Fig.2.** Optical absorption spectra recorded at 300 K for the undoped glass with $Ca_3Ga_2Ge_3O_{12}$ composition (a), the glass with $Ca_3Ga_2Ge_3O_{12}$:Mn composition containing 0.2 wt. % of Mn (b) and the glass with $Ca_3Ga_2Ge_4O_{14}$:Mn composition containing 0.15 wt. % of Mn (c).

a broad ($\Delta\lambda \cong 400 \div 600$ nm) unresolved absorption band with the maximum near 460 nm and an intense absorption in the UV region ($\lambda <$ 350 nm). The optical absorption of Mn-doped glasses is weakly dependent on temperature and its intensity is proportional to the total Mn content in samples.

The luminescence spectra of Mn-doped $CaO-Ga_2O_3-GeO_2$ glasses excited in the UV region ($\lambda_{exc}$=295 nm) manifest an intense structureless band with the halfwidth of about 3000 $cm^{-1}$ and the peak wavelength ~ 650 nm, along with a weaker complex emission band with the pronounced maximum located in the region of 380÷420 nm (see Fig. 3b, c). Another broad and weak emission band has been also observed in all the undoped $CaO-Ga_2O_3-GeO_2$ glasses (see Fig. 3a). It should be assigned to the intrinsic luminescence described for the first time in the studies [22,23]. The emission band with the maximum at ~ 650 nm observed in the Mn-doped $CaO-Ga_2O_3-GeO_2$ glasses alone (see Fig. 3b and c) might be related to Mn ions.

The optical spectra have been analysed in the framework of crystal field theory [24,25]. The excited quartet states $^4G$, $^4P$, $^4D$ and $^4F$ of $Mn^{2+}$ ions in the octahedral (cubic) crystal field are situated above the ground $^6S$ state and the trigonal crystal field splits the four levels into ten sublevels. Hence, all the transitions from the ground sextet $^6S$ to the excited levels (spin quartet or doublet) are spin-forbidden and the intensity of optical absorption lines of $Mn^{2+}$ are weak. The broad absorption band with the maximum at 460 nm is assigned to spin-allowed $^5E_g \rightarrow {}^5T_{2g}$ ($^5B_1$, $^5B_2$ and $^5A_2$) transition of $Mn^{3+}$ ($3d^4$, $^5D_0$) ions in the trigonally distorted octahedral sites of the glass network [24]. Weak spin-forbidden absorption lines of $Mn^{2+}$ ions in the octahedral sites of $CaO-Ga_2O_3-GeO_2$ glass have not been observed against the background of strong absorption band of $Mn^{3+}$. Larger $Mn^{2+}$ fractions result in more transparent glass samples, whereas larger $Mn^{3+}$ fractions yield in increasing purple colour and a red shift of the absorption saturation wavelength. An intense absorption of the Mn-doped $CaO-Ga_2O_3-GeO_2$ glasses in the UV region (at $\lambda <$ 350 nm – see Fig. 2b and c) is related to $O^{2-} \rightarrow Mn^{3+}$ charge-transfer band.

Basing on the analysis of the literature data [5,14,15,24], we can state that the intense broad emission band with the maximum near 650 nm (15000 $cm^{-1}$) (see Fig. 3 to 5) corresponds to $^4T_{1g} \rightarrow {}^6A_{1g}$ transition of $Mn^{2+}$ ions in the trigonally distorted octahedral sites of the glass network. Decrease in temperature down to the liquid nitrogen one leads to a red shift of $Mn^{2+}$

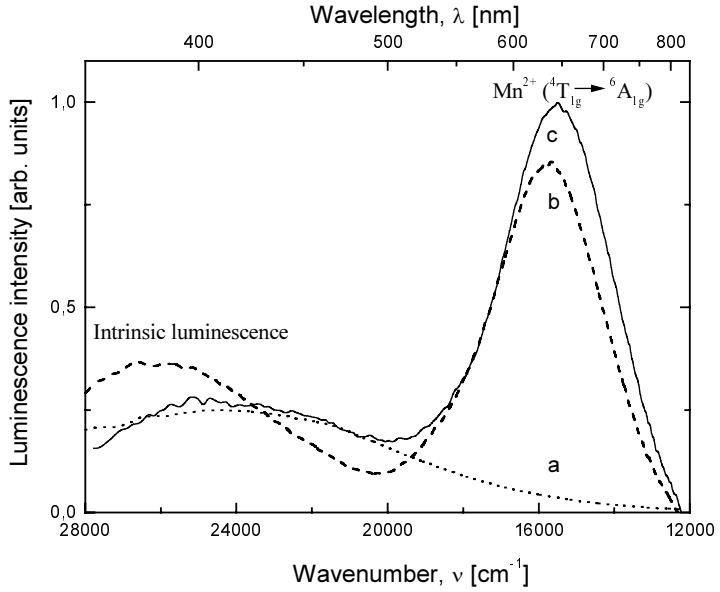


**Fig. 3.** Luminescence spectra for the undoped glass with $Ca_3Ga_2Ge_4O_{14}$ composition (a), the Mn-doped glass with $Ca_3Ga_2Ge_3O_{12}$ composition containing 0.2 wt. % of Mn (b) and the Mn-doped glass with $Ca_3Ga_2Ge_4O_{14}$ composition containing 0.15 wt. % of Mn (c). The spectra are recorded at 300 K under the excitation with $\lambda_{exc}$ = 295 nm.

luminescence band. It is worth noticing that the red shift of the $Mn^{2+}$ emission band with increasing $Mn^{2+}$ concentration has been observed in barium phosphate glasses [6]. Both of these effects are typical for $Mn^{2+}$ ions in phosphors. They can be explained by magnetic interaction between the pairs of $Mn^{2+}$ ions [26,27]. At the low temperatures, the linewidths of the $Mn^{2+}$ emission and $Mn^{3+}$ absorption bands hardly non-change, thus indicating inhomogeneous broadening of these bands caused by differing local crystal fields at the activator sites.

Following from the Tanabe-Sugano diagrams for $3d^5$-configuration [28], the luminescence excitation bands in the vicinity of 350 nm (26500 $cm^{-1}$), 420 nm (24000 $cm^{-1}$) and 500 nm (21000 $cm^{-1}$) have been assigned to $Mn^{2+}$ transitions from the ground $^6A_{1g}$ level to the levels $^4T_{2g}$ ($^4D$), $^4A_{1g}$, $^4E_g$ ($^4G$) and $^4T_{1g}$ ($^4G$), respectively (see Fig. 6). The transitions $^6A_{1g} \rightarrow {}^4T_{1g}$ ($^4G$), $^6A_{1g} \rightarrow {}^4E_{2g}$($^4D$) and $^6A_{1g} \rightarrow {}^4T_{1g}$, $^4A_{2g}$ ($^4F$) also reveal themselves in the luminescence excitation spectra of $Mn^{2+}$ (Fig. 6). Using the positions of the luminescence excitation bands, we have evaluated the average crystal field parameters for $Mn^{2+}$ ions in the octahedral sites of the glass network: the crystal field strength is equal to $Dq \cong 840$ $cm^{-1}$, the Racah parameter $B \cong 770$ $cm^{-1}$ and $Dq/B \cong 1.1$. Notice that, unlike the Mn-doped compositionally disordered Ca-gallogermanate crystals [14,15], the excitation of $Mn^{2+}$ luminescence band in $CaO\text{-}Ga_2O_3\text{-}GeO_2$ glasses is connected with the intrinsic luminescence (see Fig. 3 to 5). This result clearly demonstrates that the energy absorption and transfer processes causing the emission in the glassy compounds of

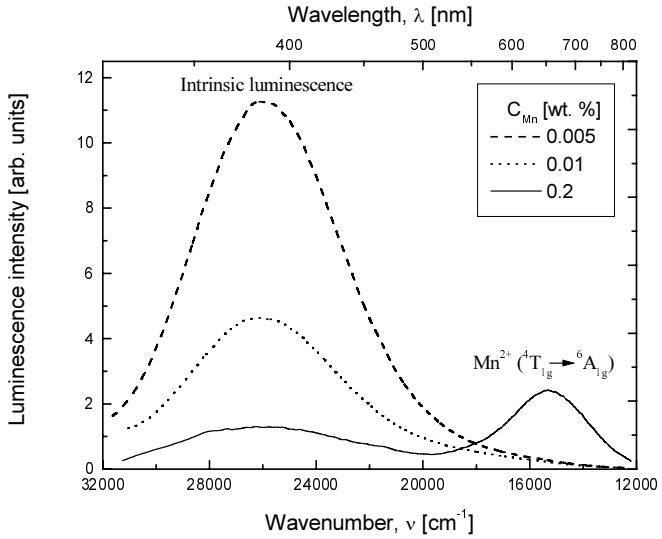


**Fig. 4.** Luminescence spectra of $Mn^{2+}$ ions in the glasses with $Ca_3Ga_2Ge_3O_{12}$ composition containing different amounts of Mn. The spectra are recorded at 300 K under the excitation with $\lambda_{exc}$ = 295 nm. The detailed description of the samples is given in the figure.

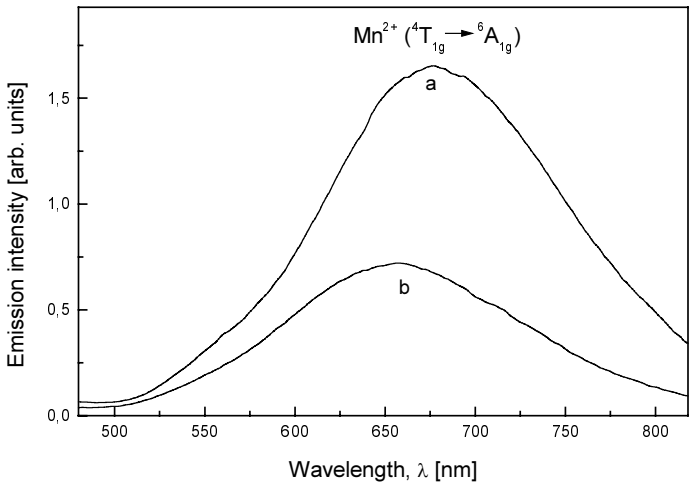


**Fig. 5.** Luminescence spectra of $Mn^{2+}$ ions in the glasses with $Ca_3Ga_2Ge_4O_{14}$:Mn composition containing 0.15 wt. % of Mn.
The spectra are recorded at 80 K (a) and 300 K (b) under the excitation with $\lambda_{exc}$ = 290 nm.

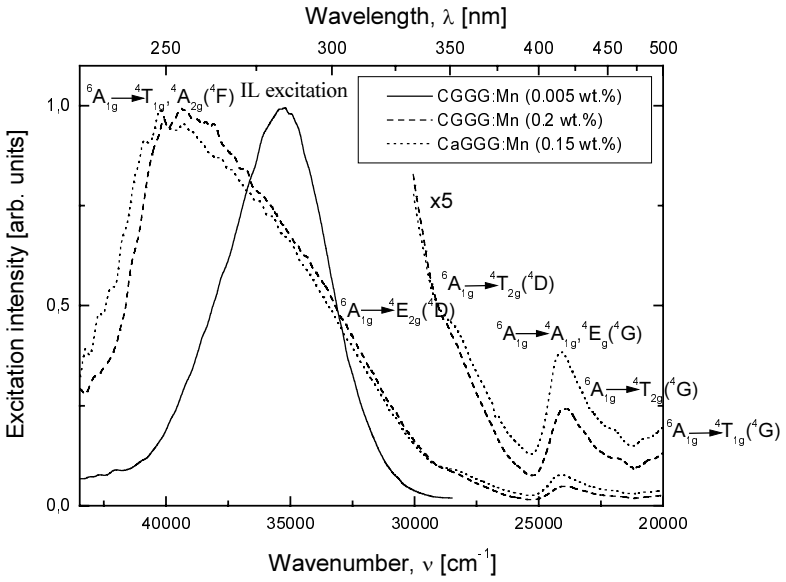


**Fig. 6.** Luminescence excitation spectra of $Mn^{2+}$ ions in the glasses with $Ca_3Ga_2Ge_3O_{12}$ composition containing 0.001 and 0.2 wt. % of Mn and the glass with $Ca_3Ga_2Ge_4O_{14}$ composition containing 0.15 wt. % of Mn. The spectra are recorded at 300 K. The detailed description of the samples is given in figure (the abbreviations CGGG and CaGGG mean the glasses with the garnet and Ca-gallogermanate compositions, respectively)..

$CaO-Ga_2O_3-GeO_2$ system are more complicated than those occurring in crystals and so they need a more detailed study.

Let us now consider in brief the peculiarities of incorporation of manganese impurity into the crystals and glasses of $CaO-Ga_2O_3-GeO_2$ system. In case of low enough Mn concentrations (less than 0.1 at. %), Mn is incorporated into the lattice of ordered calcium-gallium-germanium garnet crystals as $Mn^{4+}$ and occupies octahedral [a] sites [11,12]. Besides of $Mn^{4+}$, $Mn^{2+}$ ions in dodecahedral {c} sites of the garnet lattice have been detected by the EPR technique at higher Mn contents (more than 0.1 at. %) [13]. The main part of the Mn impurity is incorporated into the lattice of as-grown disordered Ca-gallogermanate crystals as $Mn^{3+}$ ions that substitute $Ga^{3+}$ cations in the octahedral (1a) sites [14,15]. The heat treatment of single $Ca_3Ga_2Ge_4O_{14}$:Mn crystals in vacuum at T = 1000 K gives rise to reduction of $Mn^{3+}$ ions to $Mn^{2+}$ ones [14,15]. In the network of as-synthesised $CaO-Ga_2O_3-GeO_2$ glasses, the Mn impurity is simultaneously incorporated as $Mn^{3+}$ and $Mn^{2+}$ ions in the 0.001 ÷ 0.2 wt. % concentration range. Moreover, the $Mn^{3+}/Mn^{2+}$ ratio does not change after the heat treatment in vacuum, $H_2$ and $O_2$ atmospheres. The observed peculiarities of Mn incorporation could be explained by different mechanisms of charge compensation in the ordered garnet crystals $Ca_3Ga_2Ge_3O_{12}$ [11,13], substitutionally disordered crystals $Ca_3Ga_2Ge_4O_{14}$ [14,15] and the glasses of the same compositions.

The decay luminescence curves for the $^4T_{1g} \rightarrow {}^6A_{1g}$ transition ($\lambda_{max} \cong 650$ nm) of $Mn^{2+}$ centres in the glass with $3CaO-Ga_2O_3-3GeO_2$ composition are depicted in Fig. 7. They are obtained at the room temperature and the excitation wavelengths $\lambda_{exc} = 275$ nm (Fig. 7a) and $\lambda_{exc} = 300$ nm (Fig. 7b). A comparison of one- and two-exponent fittings of the decay curves shows that the latter evidently prevails over the former. At the same time, let us note that the three-exponent model brings no further improvement. Thus, one can conclude that the decay curve observed for the $Mn^{2+}$ luminescence centres is described by the sum of two exponents, with the following lifetimes: $\tau_1 = 12.3$ ms and $\tau_2 = 4.07$ ms at $\lambda_{exc}$=275 nm and $\tau_1$=12.4 ms and $\tau_2 = 3.98$ ms at $\lambda_{exc} = 300$ nm. According to [6], the longer decay time $\tau_1$ could be assigned to the isolated (single) $Mn^{2+}$ luminescence centres in the octahedral sites, whereas the shorter one, $\tau_2$ , refers to the pairs (or small clusters) of $Mn^{2+}$ centres. The analysis of the decay time evidences that the number of isolated $Mn^{2+}$ centres in the $CaO-Ga_2O_3-GeO_2$ glass network is approximately equal to 64%, while

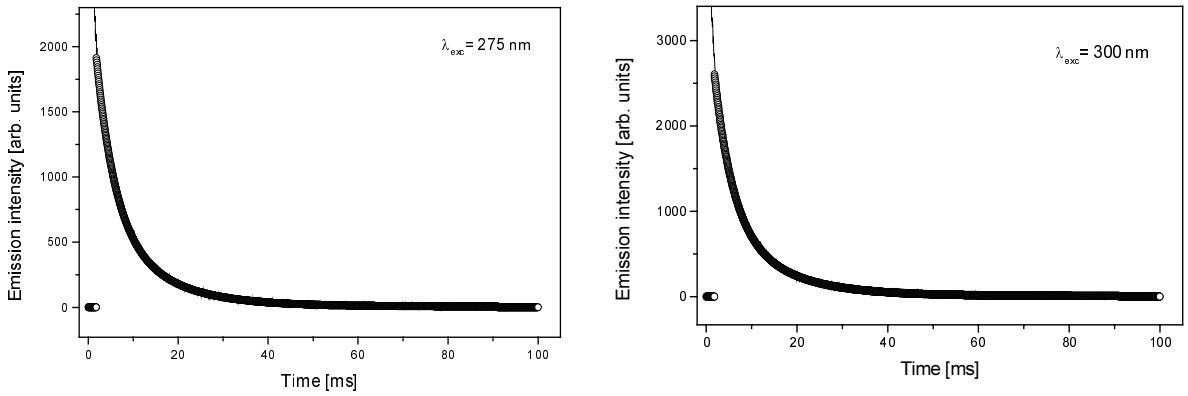


**Fig. 7.** Decay curves for $Mn^{2+}$ luminescence centres ($^4T_{1g} \rightarrow {}^6A_{1g}$ transition) for the glasses with $Ca_3Ga_2Ge_4O_{14}$ composition containing 0.15 wt. % of Mn. The decay curves are registered at 295 K under the excitation with $\lambda_{exc}$ = 275 nm (a) and $\lambda_{exc}$ = 300 nm (b). Open circles refer to the experiment and solid lines represent the result of the two-exponent fit (see the text).

that of the $Mn^{2+}$ pairs (or the small clusters) is about 36%.

The analysis of the luminescence kinetics presented here demonstrates also a good correlation with the EPR spectroscopy data. In the Mn-doped glasses of $CaO\text{-}Ga_2O_3\text{-}GeO_2$ system, two types of $Mn^{2+}$ luminescence centres actually exist, which manifest essentially different lifetimes. The first type represents an ensemble of isolated $Mn^{2+}$ centres with statistically distributed parameters in the octahedral sites of the glass network. The second one corresponds to the pairs and small clusters of $Mn^{2+}$ centres coupled via the magnetic exchange interaction.

Let us stress that the EPR, magnetic susceptibility and the luminescence decay measurements [16,29] have also ascertained availability of two different types of $Cr^{3+}$ luminescence centres in the glass with $3CaO\text{-}Ga_2O_3\text{-}3GeO_2$ or $Ca_3Ga_2Ge_3O_{12}$ garnet compositions. Nonetheless, both types of $Cr^{3+}$ centres refer to the isolated ions, in contrast to the $Mn^{2+}$ centres. The local environments for the two different types of luminescence $Mn^{2+}$ and $Cr^{3+}$ centres in the glasses of $CaO\text{-}Ga_2O_3\text{-}GeO_2$ system need a more detailed study. This will be reported in a separate work, enabled after the analysis *K*-edge of EXAFS (Extended X-ray Absorption Fine Structure) spectra for Mn and Cr obtained at DESY HASYLAB (Hamburg, Germany).

## Conclusions

Basing on the analyses of the EPR and optical spectroscopic data, we draw the following conclusions:

1. The manganese is incorporated as $Mn^{2+}$ and $Mn^{3+}$ ions into the trigonally distorted octahedral sites of the $CaO\text{-}Ga_2O_3\text{-}GeO_2$ glass network. The observed EPR and optical spectra of the Mn-doped glasses of $CaO\text{-}Ga_2O_3\text{-}GeO_2$ system are almost independent of the basic glass composition. They reveal all the features characteristic of the glassy state (a presence of low-symmetry centres of several types, broad distribution of crystal field parameters and inhomogeneous broadening of the spectral lines).
2. The intense broad absorption band with the maximum near 460 nm is related to the spin-allowed $^5E_g \rightarrow {}^5T_{2g}$ transition of $Mn^{3+}$ ions in trigonally distorted octahedral sites of the $CaO\text{-}Ga_2O_3\text{-}GeO_2$ glass network. The absorption in the UV region is associated with $O^{2-} \rightarrow Mn^{3+}$ charge-transfer band. The spin-forbidden weak absorption lines of $Mn^{2+}$ ions have not been observed against the background of strong absorption band peculiar for $Mn^{3+}$.

3. The emission band with the maximum in the vicinity of 650 nm (15000 $cm^{-1}$) may be satisfactorily explained in the framework of $Mn^{2+}$ transitions in trigonally distorted octahedral sites as being due to $^4T_{1g} \rightarrow {}^6A_{1g}$ transition. The excitation of red $Mn^{2+}$ luminescence leads to decreasing intensity of the intrinsic violet-blue luminescence in the $CaO-Ga_2O_3-GeO_2$ glasses. This feature is linked to transfer of the excitation energy from the intrinsic luminescence centres to the impurity $Mn^{2+}$ centres.
4. The luminescence decay curves of $Mn^{2+}$ (the $^4T_{1g} \rightarrow {}^6A_{1g}$ transition) measured at the room temperature may be well described within the two-exponent approximation, using the lifetimes $\tau_1$=12.3 and $\tau_2$=4.07 ms for $\lambda_{exc}$ = 275 nm and $\tau_1$=12.4 and $\tau_2$=3.98 ms for $\lambda_{exc}$ = 300 nm. They correspond respectively to the $Mn^{2+}$ centres isolated in octahedral sites and the magnetic-coupled $Mn^{2+}$ pairs (or small $Mn^{2+}$ clusters) in the $CaO-Ga_2O_3-GeO_2$ glass network. The EXAFS studies of the local environments for different $Mn^{2+}$ centres in $CaO-Ga_2O_3-GeO_2$ glasses are now in progress.
5. The results of optical studies presented here testify that the glasses of $CaO-Ga_2O_3-GeO_2$ system, when activated with $Mn^{2+}$ ions, could represent promising materials for the efficient red phosphors.

## Acknowledgements

The authors are grateful to P.Buchynskii from the Lviv Scientific Industrial Amalgamation “MikroTech Karat” (Ukraine) for synthesis of the glass samples. This work has been partly supported by Kazimierz Wielki University of Bydgoszcz under the Grant BW/2005.

## References

1. Shionoya S. and Yen W.M. Phosphor handbook, Chapter 3, CRS Press, Boca Raton, FL (1999).
2. Blasse G. and Bril A. Philips Tech. Rev. **31** (1970) 304.
3. Qiu J., Zhu C., Nakaya T., Si J., Kojima K., Ogura F. and Hirao K. Appl. Phys. Lett. **79** (2001) 3567.
4. Reisfeld R., Kisilev A. and Jorgensen C.K. Chem. Phys. Lett. **111** (1984) 19.
5. Faber A.J., van Die A., Blasse G. and van der Weg F. Phys. Chem. Glasses **28** (1987) 150.
6. Machado I.E.C., Prado L., Gomes L., Prison J.M. and Martinelli J.R. J. Non-Cryst. Solids **348** (2004) 113.
7. Damen J.P.M., Pistorius J.A. and Robertson J.M. Mater. Res. Bull. **12** (1977) 73.
8. Mill B.V., Butashin A.V., Ellern A.M. and Majer A.A. Izv. Akad. Nauk SSSR, Ser. Neorg. Mater. **17** (1981) 1648 (in Russian).
9. Padlyak B.V. and Buchynskii P.P. Patent of Ukraine No. UA 25235 A, October 30, 1998.
10. Padlyak B., Mudry S., Halchak V., Korolyshyn A., Rybicki J. and Witkowska A., Opt. Appl. **30** (2000) 691.
11. Nosenko A.E., Padlyak B.V. and Kravchishin V.V. Sov. Phys.: Solid State **27** (1985) 2083.
12. Nosenko A.E., Abramov A.P., Kostyk L.V., Bily A.I. and Kravchishin V.V. Opt. Spektrosk. **61** (1986) 1037 (in Russian).
13. Padlyak B.V. and Nosenko A.E. Sov. Phys.: Solid State **30** (1988) 1027.
14. Nosenko A.E., Leshchuk R.Ye. and Padlyak B.V. Zhurn. Prikl. Spektrosk. **59** (1993) 146 (in Russian).
15. Nosenko A.E., Leshchuk R.Ye. and Padlyak B.V. Radiation Effects and Defects in Solids **135** (1995) 55.
16. Padlyak B.V. and Gutsze A. Appl. Magn. Reson. **14** (1998) 59.
17. Padlyak B., Kukliński B. and Grinberg M. Proc. International Congress on Glass, V. **2**, Edinburgh, Scotland (2001) 773.
18. Padlyak B.V., Kukliński B. and Grinberg M. Phys. Chem. Glasses C **43** (2002) 392.
19. Loveridge D. and Parke S. Phys. Chem.

Glasses **12** (1971) 19.
20. Griscom D. L. J. Non-Crystal. Solids **40** (1980) 211.
21. Brodbeck C.M. and Bukrey R.R. Phys. Rev. B **24** (1981) 2334.
22. Padlyak B.V., Bordun O.M. and Buchynskii P.P. Acta Phys. Polon. A **95** (1999) 921.
23. Padlyak B.V. and Kukliński B. Radiat. Meas. **38** (2004) 593.
24. Sviridov D.T., Sviridova R.L. and Smirnov Yu.F. Optical spectra of transition metal ions in crystals, Nauka, Moscow, 1976 (in Russian).
25. Henderson B. and Bartram R.H. Crystal-field engineering of solid-state laser materials, Cambridge University Press, Cambridge, 2000.
26. Vink A.P., de Bruin M.A., Roke S., Peijzel P.S. and Meijerink A. J. Electrochem. Soc. E **148** (2001) 313.
27. Ronda C.R. and Amrein T. J. Lumin. **69** (1996) 245.
28. Tanabe Y. and Sugano S. J. Phys. Soc. Japan **9** (1954) 753; Tanabe Y. and Sugano S. J. Phys. Soc. Japan **9** (1954) 766.
29. Padlyak B.V., Koepke Cz., Wisniewski K., Grinberg M., Gutsze A. and Buchynskii P.P. J. Lumin. **79** (1998) 1.